



Research Article

Spectral-Temporal Optical Code Division Multiple Access Code for High Capacity Passive Optical Networks

Mansoor Qadir^{1*}, Yousaf Khan², Shahid Khan³, Djamaledine Djeldjli³ and Muhanned Ismael Ibrahim Al Firas⁴

¹Department of Computer Science, Iqra National University, Peshawar 25000, Pakistan; ²Department of Electrical Engineering, Iqra National University, Peshawar 25000, Pakistan; ³Institut Supérieur d'Électronique et d'Automatique, University De Lorraine, 57070, France; ⁴Department of Electrical Engineering, President, Gulf University, Kingdom of Bahrain.

Abstract: Optical code division multiple access (OCDMA) techniques have attracted much attention by allowing each communicating subscriber's simultaneous access of the entire medium with maximum security and spectral efficiency. This paper aims to design and analyze 2 dimensional OCDMA based coding scheme and corresponding network architecture to support high capacity Gigabit Passive Optical Network (GPON). The coding scheme is proposed by deploying diagonal eigenvalue unity (DEU) scheme at the frequency domain (X-axis) in combination with double weight zero cross-correlation (DW-ZCC) code at the time domain (Y-axis). The proposed 2D-DZ coding scheme provides high orthogonality in adjacent codes and resolves the problem of larger code lengths. The new coding scheme and corresponding network architecture is analyzed in terms of Gaussian Approximation analysis and simulation through OptiSystem. It is observed that the proposed 2D-DZ based OCDMA system supports data rate of up to 2 Gbps for relatively large number of subscribers and extended reach in comparison with the existing counterparts.

Received: March 13, 2020;; **Accepted:** May 03, 2020;; **Published:** June 30, 2020

***Correspondence:** Mansoor Qadir, Department of Computer Science, Iqra National University, Peshawar 25000, Pakistan; **Email:** mansoor.qadir@hotmail.com

Citation: Qadir, M., Y. Khan, S. Khan, D. Djeldjli and M.I.I. Al Firas. 2020. Spectral-temporal optical code division multiple access code for high capacity passive optical networks. *Journal of Engineering and Applied Sciences*, 39(1): 103-115.

DOI: <http://dx.doi.org/10.17582/journal.jeas/39.1.103.115>

Keywords: Two dimensional codes, Optical code division multiple access, Diagonal eigenvalue unity, Zero cross correlation

Introduction

Optical CDMA systems have caught significant attention since their inception owing to use of asynchronous transmission, unique coding schemes, and relatively simple network architecture. OCDMA based systems are readily adapted in passive optical networks (PONs) for the provision of high bandwidth with relatively low cost of deployment. However, such schemes limit system's output and its performance due to one dimensional (1D) nature of this coding schemes. Such factor introduces several problems in OCDMA based PONs that limits the addition of new subscribers communicating at large data rates suggested by (Ghafouri-Shiraz and Karbassian, 2012;

Nisar, 2014; Lam, 2011), Passive optical networks: Principles and practice (Elsevier and Koonen, 2006; Azizoglu *et al.*, 1992; Lee *et al.*, 2001).

Other than that 2D coding schemes were introduced to overcome the problems in conventional 1D codes. 2D-OCDMA codes add an extra dimension to the exiting coding schemes in order to reduce the impact of code length with increase in the number of users according to (Kumawat *et al.*, 2017; Yin and Richardson, 2009; Abdullah *et al.*, 2012; Kandouci *et al.*, 2017; Singh *et al.*, 2016; Najjar, 2017; Ahmed *et al.*, 2019).

Shi and Ghafouri-Shiraz (2016) suggested that

such technique improves the orthogonality between adjacent codes that helps in the recovery of transmitted information at the receiving end such that the auto correlation is maximum i.e. equal to the code weight and the cross correlation is as low as 0 or 1 to reduce the impact of communicating subscriber with the intended information.

2D-OCDMA systems are constructed utilizing the frequency in spectral domain and amplitude in spatial domain i.e. spectral-spatial technique which uses parallel optical fiber paths in addition with spectral encoding-decoding for high capacity.

Ahmed, 2013; Anuar *et al.*, 2009; Mahloo, 2013; Anuar *et al.*, 2013; Sahbudin *et al.*, 2013 the inherent nature of spatial encoding is the major limiting factor for the deployment of such systems. The spatial coding scheme required numerous optical fibers which increases the deployment cost which marks it incongruous for adopting such systems in the access network GPON when the requirement is lowering the cost of implementation.

In quest to overcome the problem of parallel fiber strands, spectral-temporal encoding is adapted to limit the overall cost of deployment. However, utilization of the time-based encoding and decoding can limit the amount of data carrying capacity for the network. Therefore, it is of prime significance to determine a suitable coding scheme that can address the issue with minimum impact on system cost.

This manuscript adapts the blend of diagonal eigenvalue unity (DEU) and zero cross correlation

(ZCC) code along the spectral and temporal domain respectively. Combination of both codes are utilized to develop a 2D code called 2D-DZ code with efficient performance parameters in comparison with the existing counterparts. The proposed code is analyzed through comprehensive mathematical formulism through Gaussian Approximation analysis as recommended by Kandouci, 2017. Shi and Ghafouri-Shiraz (2016) and Ahmed and Nisar (2013) recommended three noise sources for the code capacity analysis i.e. intensity, thermal and shot noise are considered at higher data rates in order to support the maximum number of users w.r.t performance parameter of BER. The analysis in this work illustrates not only improved transmission capacity of the system yet the simplified proposed 2D-DZ OCDMA system architecture makes it more suitable for the deployment of GPONs at the low-cost access domain in comparison with the other coding schemes.

Table 1 shows a detailed comparison of Spectral/spatial and spectral/temporal coding techniques based on of transmission capacity, received power, encoder and architecture complexity.

Design of 2D-DZ coding scheme

In order to generate a coding scheme with most efficient properties, in terms of code length (L), hamming weight (w), and auto- (λ_a) and cross-correlation (λ_c), the propose model employs 1D SAC-OCDMA coding schemes namely DEU and ZCC codes respectively (14, 15). Table 2 shows the 1D DEU and ZCC chips distribution for 4 users with $w_{DEU} = 3$ and $L_{DEU} = [N_{DEU}(w_{DEU} - 1) + 1]$ and $w_{ZCC} = 2$ and $L_{ZCC} = [N_{ZCC} \times w_{ZCC}]$, respectively (17, 19, 31, 32).

Table 1: Comparison of various 2D OCDMA techniques.

Spectral-spatial code sequences					
Code Name	Spectral and spatial code seq	Transmission capacity	Received power (dBm)	Encoder decoder complexity	Architecture complexity
2D-DCS	Sr = 57 Si = 3	622 Mbps at 171	0	Complex	Moderate
	Sr = 21 Si = 7	622 Mbps at 285		Complex	Complex
2D-DEU	Sr = 15 Si = 9	2.5 Gbps at 90	-10	Complex	Complex
2D-MS	Sr = 57 Si = 3	622 Mbps at 171	-10	Complex	Moderate
	Sr = 24 Si = 6	622 Mbps at 220		Complex	Complex
2D-DPD	Sr = 57 Si = 3	1 Gbps at 132	0	Complex	Complex
2D-EEEMD	Sr = 63 Si = 3	2 Gbps at 192	-10	Complex	Moderate
2D-FRS	Sr = 63 Si = 3	622 Mbps at 128	0	Complex	Moderate
Wavelength-Temporal code sequences					
2D-W/T-MQC/MQCs	Sr = 30 Te = 30	622 Mbps at 625	10	Complex	Moderate
2D ZCC/ZCC	Not Given	2.5 Gbps at 4	Not Given	Moderate	Simple
2D-PCBD	Sr = 15 Te = 7	622 Mbps at 115	Not Given	Moderate	Simple

Table 2: Construction and spectral allocation of 1D DEU and ZCC codes.

Users	1D-DEU									
	λ_1	λ_2	λ_3	λ_4	λ_5	λ_6	λ_7	λ_8	λ_9	PoS
1	1	1	1	0	0	0	0	0	0	[1, 2, 3]
2	0	0	1	1	1	0	0	0	0	[3, 4, 5]
3	0	0	0	0	1	1	1	0	0	[5, 6, 7]
4	0	0	0	0	0	0	1	1	1	[7, 8, 9]
1D-ZCC										
1	1	1	0	0	0	0	0	0		[1, 2]
2	0	0	1	1	0	0	0	0		[3, 4]
3	0	0	0	0	1	1	0	0		[5, 6]
4	0	0	0	0	0	0	1	1		[7, 8]

Now for the proposed 2D-DZ code, 1D DEU code is utilized across the spectral domain or X-axis (X^{th} code sequence). Whereas, 1D ZCC code is used along the time domain or Y-axis (Y^{th} code sequence). This arrangement significantly improves the orthogonality/ correlation between adjacent codes and reduces the impact of interfering users at the receiving photodiode. Table 3 demonstrates X^{th} and Y^{th} sequences that are utilized from Table 3.

Table 3: Spectral and temporal code sequences for the proposed 2D-DZ code.

X^{th} code sequences	Y^{th} code sequences
$X_1 = \{111000000\}$	$Y_1 = \{11000000\}$
$X_2 = \{001110000\}$	$Y_2 = \{00110000\}$
$X_3 = \{000011100\}$	$Y_3 = \{00001100\}$
$X_4 = \{000000111\}$	$Y_4 = \{00000011\}$

Table 4: Code matrices for the proposed 2D-DZ coding scheme.

$A_{g,h} = Y_h^T X_g$	$X_1 = [111000000]$	$X_2 = [001110000]$
Y_1^T	$\begin{bmatrix} 111000000 \\ 111000000 \\ 000000000 \\ 000000000 \\ 000000000 \\ 000000000 \\ 000000000 \\ 000000000 \\ 000000000 \end{bmatrix}$	$\begin{bmatrix} 001110000 \\ 001110000 \\ 000000000 \\ 000000000 \\ 000000000 \\ 000000000 \\ 000000000 \\ 000000000 \\ 000000000 \end{bmatrix}$
Y_2^T	$\begin{bmatrix} 000000000 \\ 000000000 \\ 111000000 \\ 111000000 \\ 000000000 \\ 000000000 \\ 000000000 \\ 000000000 \\ 000000000 \end{bmatrix}$	$\begin{bmatrix} 000000000 \\ 000000000 \\ 001110000 \\ 001110000 \\ 000000000 \\ 000000000 \\ 000000000 \\ 000000000 \\ 000000000 \end{bmatrix}$

Suppose g^{th} and h^{th} code sequences for X and Y are X_g and Y_h , where $g = 0, 1, 2 \dots N_{DEU-1}$ and $h = 0, 1,$

$2 \dots N_{ZCC-1}$. Then, the proposed 2D-DZ code can be expressed as the combination of X_g and X_b^T , where Y_b^T represents the transpose of Y_b code, respectively (24). Now the resulting code with length $L = L_{DEU} \times L_{ZCC}$ can be written as;

$$D_{g,h} = Y_h^T X_g \dots (1)$$

The proposed 2D-DZ codes from the combination of X and Y code sequences are shown in Table 4.

Cross correlation values for 2D-DZ code

It is of primal importance to determine the cross-correlation properties of the proposed code in order to determine its suitability for the support of high transmission capacity through the mitigation of noise from interfering subscribers. Moreover, it will also help to design a suitable encoder and decoder to ensure an efficient operation of the system. Thus, four characteristic matrices are identified to determine the cross correlation, λ_c values for the proposed 2D-DZ code encoded spectrum after recovery at the PIN photodiode. The four matrices are developed by undertaking all possible arrangement of X_g and Y_h codes sequences, which can be written as:

$$\begin{aligned} E_{g,h}^{(0)} &= Y_h^T X_g \\ E_{g,h}^{(1)} &= Y_h^T \bar{X}_g \\ E_{g,h}^{(2)} &= Y_h^T X_g \\ E_{g,h}^{(3)} &= \bar{Y}_h^T \bar{X}_g \dots (2) \end{aligned}$$

Now \bar{X}_g and \bar{Y}_g^T in Equation 2 are the complementary codes of spectral and temporal code sequences respectively. Consequently, the resulting λ_c between E^d and $E_{g,b}$ for the proposed 2D-DZ code based on the characteristic matrices can be expressed as

$$C^{(d)}(g, h) = \sum_{i=1}^{L_{ZCC}} \sum_{j=1}^{L_{DEU}} e_{(i,j)}^{(d)} e_{(i,j)}(g, h) \dots (3)$$

Where $e_{(i,j)}^{(d)}$ and $e_{(i,j)}$ demonstrates the elements from characteristic matrix E^d and $E_{g,b}$, respectively. Now, the λ_c values for the proposed 2D-DZ codes are listed in Table 5.

Table 5 shows that λ_c only exists along the X^{th} code sequences, so the four characteristic matrices can be rearranged into two new groups constructed as:

$$C_{g,h}^{(0-2)} = \{C_{g,h}^{(0)}; C_{g,h}^{(2)}\} \dots (4)$$

$$C_{g,h}^{(1-3)} = \{C_{g,h}^{(1)}; C_{g,h}^{(3)}\} \dots (5)$$

Based on the relations of $C_{g,h}^{(d-2)}$, and $C_{g,h}^{(1-3)}$, it is observed that $C_{g,h}^{(1-3)}$ correlation function have no significant contribution that significantly simplifies the detection of the intended spectrum via single balanced detector (with two photodiodes) in comparison with conventional architectures that utilizes two balanced detectors to overcome the adjacent interference. However, the noise at the receiving photodiode can be reduced by deployment of two photodiodes in single balanced detector. Thereby elevates the signal to noise ratio and quality of the received signal. The cross correlation expression becomes

$$C_{g,h}^{(0)} - \frac{C_{g,h}^{(2)}}{(w_{DEU} - 1)} = \begin{cases} w_{DEU} w_{ZCC} & \text{for } g = h = 0 \\ 0 & \text{otherwise} \end{cases} \dots (6)$$

Table 5: Cross correlation properties of the proposed 2D-DZ code.

Eg, h	$C^{(0)}(g, h)$	$C^{(1)}(g, h)$	$C^{(2)}(g, h)$	$C^{(3)}(g, h)$
$g = 0, h = 0$	w_2, w_1	0	0	0
$g \neq 0, h = 0$	w_2	0	$(w_1 - 1) w_2$	0
$g = 0, h \neq 0$	0	w_2, w_1	0	0
$g \neq 0, h \neq 0$	0	W_{ZCC}	0	$(w_1 - 1) w_2$

Proposed architecture

This section outlines design of the 2D OCDMA network architecture that is developed with 2D-DZ code. The basic building blocks of PON includes Optical Line Terminal (OLT), Optical Distribution Network (ODN) and Optical Network Termination (ONT). 32x4 matrix dimension is implemented to propose this 2D-DZ coding scheme architecture, where 32 represents the value of N_{DEU} and 4 is for the representation of N_{ZCC} values. Moreover, a hybrid topology is employed for development of the proposed architecture to exploit built-in redundancy feature that allows the traffic to flow in both direction using ring topology between OLT and ODN at FF level and also ensures better transmission capacity at access domain at the DF level Ahmed and Zeghid *et al.* (2020). The proposed architecture building blocks are:

Central office

Central office (CO) is located at the service provider.

CO is constructed utilizing combination of OLT and transmitter components i.e. encoding/decoding devices in order to effectively produce signals from the OLT to customer premises and vice versa. Moreover, CO houses switching to utilize the effective redundant nature of the ring topology and ensure network survivability at the feeder level that is more prone to fiber cuts and failures. Each block of the CO is further discussed as under.

OLT: OLT module is accountable for creating and controlling all services across the network. For the downlink traffic OLT employs a combination of light emitting diode (LEDs) as an optical carrier to transport the signal over optical distribution network (ODN)

Imtiaz *et al.* (2019) and Imtiaz *et al.* (2020) recommended LEDs are employed because they provide a relatively broad spectrum that can be used for efficient translation of binary 1's in the 2D-DZ coding scheme, into spectral representation spectral carriers via simple components like simple band pass filters.

Consequently, 30nm LED is employed at a single OLT port by translation of binary 1's in X^{th} code sequences with $g = 0, 1, 2, 3, \dots, 31$ for producing the desired signal spectrum. End-face of the LED feeds the erbium doped fiber amplifier (EDFA) arrangement in order to compensate the power drop at the next stage of splitting.

For utilization of the LED's spectrum at respective spectral encoders, end-face of the EDFA is fed to a $1:N_{DEU}$ optical power splitter (OPS) with $N_{DEU} = 32$. The amplified spectrum are forwarded to each subscriber for modulation and necessary spectral encoding inside the OLT module. For single user each leg of the optical splitter is fed to modulation arrangement that is formed by the combination of Mach-Zehnder Modulator (MZM), user's data source, and a relative line coding scheme. MZM is employed to modulate the user's data and converts the signal from electrical to optical domain as shown in Figure 1. Here the spectral encoding technique is used after signal modulation by converting the binary 1 position code sequences to X_g .

Spectral encoder: Spectral encoder comprising a single bandpass filter centered to pass the required

spectrum. As the chips are adjacent in the DEU coding scheme presented by Ahmed and Nisar (2013), in X^{th} coding sequence so single bandpass filter is used for encoding operation. For instance, if a bandpass filter with 0.4nm bandwidth is used to encode a single chip, then a filter with 1.2nm bandwidth can encode 3 adjacent chips as shown in Figure 2. This can reduce the number of filters in encoding operation of the DEU coding scheme and increases efficiency of the process since no added components are used in spectral encoding.

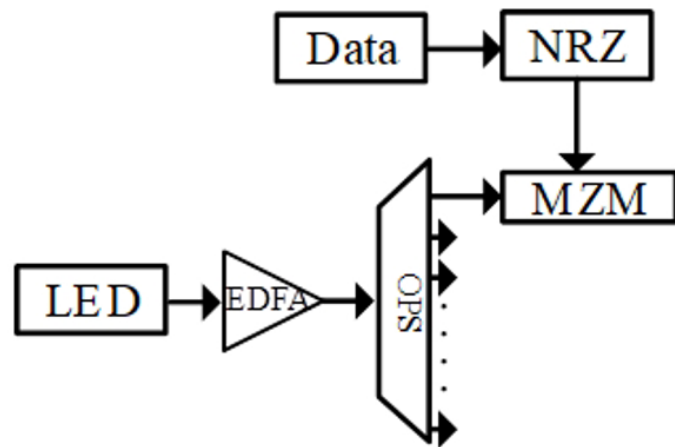


Figure 1: Modulation arrangement for a single user in proposed OLT.

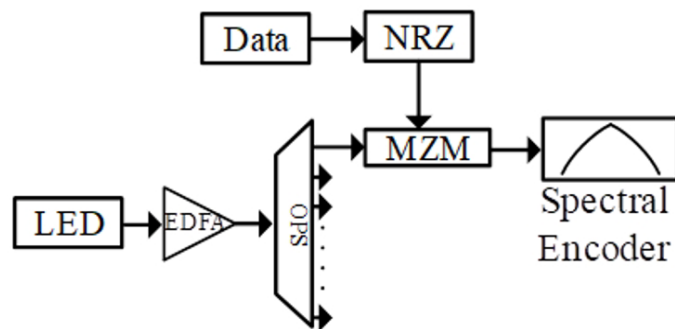


Figure 2: Spectral encoding arrangement for a single user with a single bandpass filter.

Performance of the proposed spectral encoder is evaluated for satisfactory performance in comparison with the conventional spectral encoder. Evaluation is performed at 1 Gbps of data with reference to eye diagrams at the receiving end. Eye openings in Figure 3 indicates same performance of the spectral arrangements for an acceptable BER of 10^{-9} . Consequently, the proposed architecture employs a single bandpass filter due to its satisfactory performance and relatively simple architecture.

Temporal encoder: Time-based encoder is the second stage of encoding operation that is used to

delay the spectral encoded spectrum, in reference to chip's placement in the DW-ZCC coding scheme presented by (Anuar *et al.* 2009; Qadir *et al.*, 2020). For this operation, output from the spectral encoder is split into $W_{zcc} = 2$ equal portions as shown in Figure 4. Each leg of the optical splitter is then applied to a Time Delay Unit (TDU). TDU is used to introduce the necessary time delay and is configured with reference to position chips in Y^{th} code words respectively. For instance, the code word Y^{th} has chips at the position of {1, 2} respectively. Now for a time delay unit τ_d , the delay time of the first temporal encoder will be $(1\tau_d, 2\tau_d)$, respectively. Here $\tau_d = t_d/S$, where t_d represents the bit period used for the analysis and can be written as $(1/Bit\ rate)$ and S gives the total number of time slots respectively. For four OLT ports, the value of $S = 1, 2, 3, \dots, 8$, since two TDUs are employed per PON. Output of the temporal encoder is connected to an optical circulator which is further connected to a combination of $N_{DEU}:1$. $N_{DEU}:1$ Optical Coupler (OPCU) is utilized to combine the encoded spectrums from all users and transmit them over the ODN. Consequently, the arrangement under discussion can accommodate 128 users with simultaneous access to the medium. The proposed architecture can accommodate more users as per the analytical analysis, however, a smaller number of users are taken into account to make the model realizable in OptiSystem.

Switching arrangement

Switching arrangement is employed to elevate redundancy across the feeder level and increase connection availability of the proposed model. Switching arrangement primarily employs a combination of 1:2 OPCU as shown in Figure 5. Upper leg of the OPCU is connected to the ring topology feeder level fiber, whereas the lower leg is connected to 1:2 optical switch OS with one input and two output ports. Input port of the OS is used to receive the downlink signal and forward it towards the output ports for further transmission. The output ports can be classified into port 1 (P_1) and port 2 (P_2). P_1 is connected to an optical ground, whereas P_2 is connected to other end of the ring-based fiber that is terminated into the CO.

Optical distribution network

Optical distribution network includes the components that are deployed outside the CO. For effective discussion of the ODN architecture, the proposed model is split into 3 portions, to mimic a ring based

GPON, called Feeder Level (FL), Remote Node (RN), and Distribution Level (DL)

high capacity responsible for the communication of multiplexed data from OLT towards the subscriber's module through RN. The proposed architecture adapts ring-based architecture at the feeder level to offer relatively high-level redundancy at low costs in comparison with tree-based counterparts.

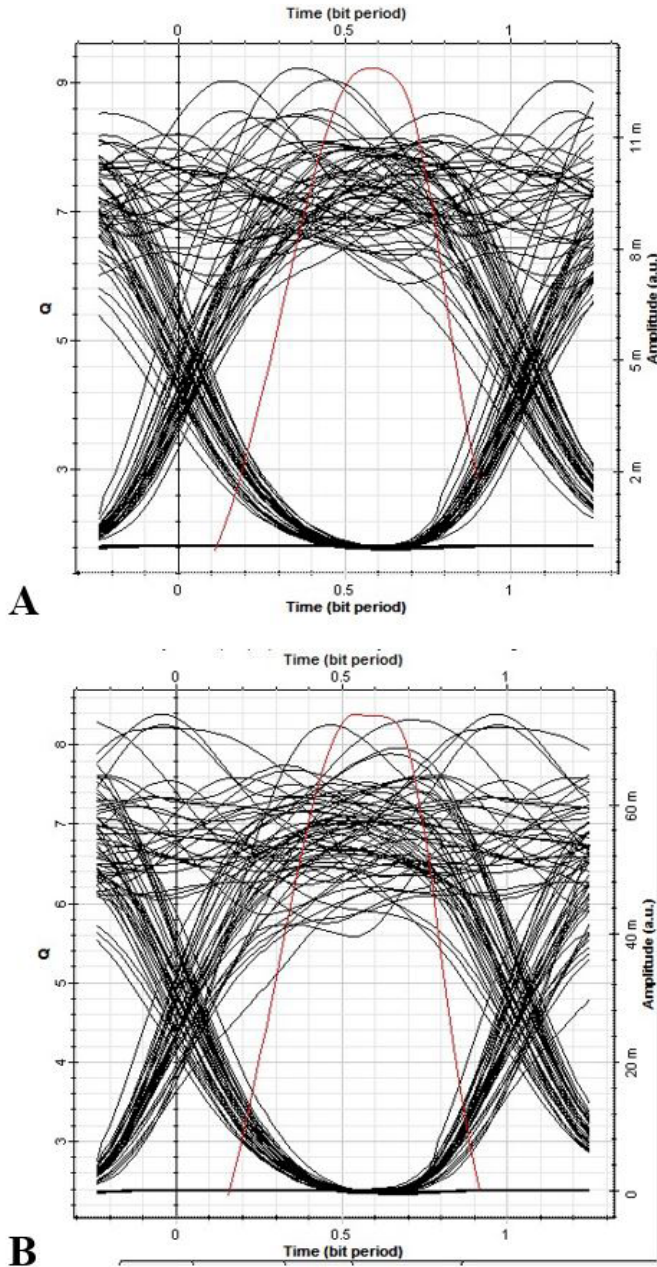


Figure 3: Eye diagrams for both Mux based encoder and proposed single bandpass filter-based encoder.

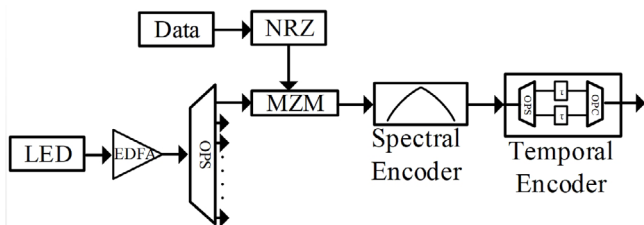


Figure 4: Proposed 2D-DZ architecture with spectral and temporal encoding.

Feeder level: Feeder level (FL) covers the deployment of optical fiber media from CO till the RN. It primarily employs a long span optical fiber media with relatively

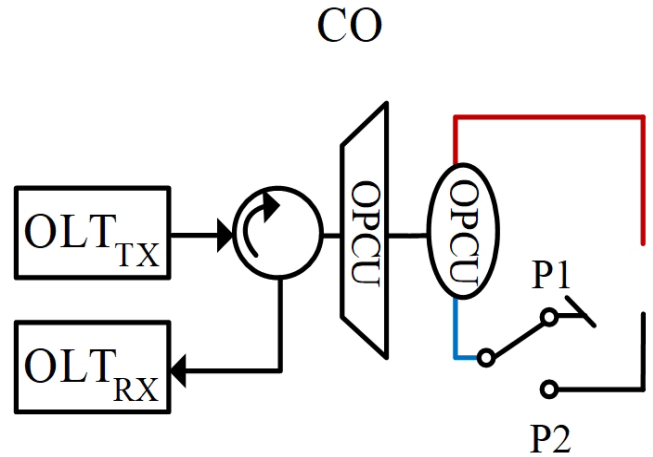


Figure 5: Proposed switching arrangement for redundancy.

The proposed model consists of a high capacity light-wave path that is connected to port P_1 of the switching arrangement at one end and terminates at the first remote node RN_1 . Since ring-based architecture suffer from power budget issues, therefore, an effective number of RNs is introduced to serve the given number of users accessing the medium simultaneously. The number of RNs required for the proposed architecture is equivalent to the value of h , and each RN can serve a total of N_{DEU} subscribers.

Remote nodes: Each RN is formed by the combination of two power couplers with symmetric split ratio throughout the feeder level. Now, feeder fiber is received by each remote node through a 1:2 $OPCU_{RNb}$ with one input and 2 output ports as shown in Figure 6. For the purpose of demonstration, first remote node (1:2 $OPCU_{RNb}$) is considered with input port as "a", and the upper and lower output ports as "b" and "c" respectively. Now the encoded and multiplexed signal received at port a of 1:2 $OPCU_{RN1}$ is split into two equal portions. One portion of the signal is fed to $OPCU_{RN1}$, via port b, with a split ratio of 1: N_{DEU} . Whereas, another portion is forwarded towards the adjacent remote node (RN_2) through port c.

$OPCU_{RN1}$ effectively splits the encoded and multiplexed signal into N_{DEU} equal portions. Each split portion is carried to the intended subscriber's ONT through short span distribution fibers (DF).

Since the number of $OPCU1_{RN1}$ used throughout the network is translated by the value of b in Y^T_b code word respectively. Therefore, it is of primal importance to keep the number of codes as less as possible to address the power constraints of the ring-based topology.

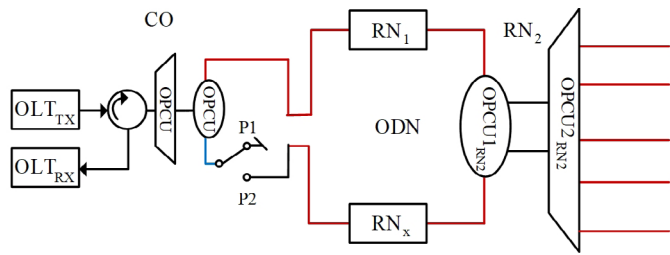


Figure 6: Proposed 2D-DZ OCDMA system with OLT rack and RN's arrangement.

Optical network terminal: ONT module for the proposed 2D-DZ based OCDMA systems initiates with a time-based decoder arrangement that employs a 1:2 power splitter to split the incoming signal into 2 equal portions. Each split portion of the optical power splitter is connected to TDU that is configured through $(S-1-j)$, where j is the chip position in the Y^T_b code sequence (10). Received signals after passing through the TDUs are combined and forwards towards the spectral decoder through a 2:1 power combiner as shown in Figure 7.

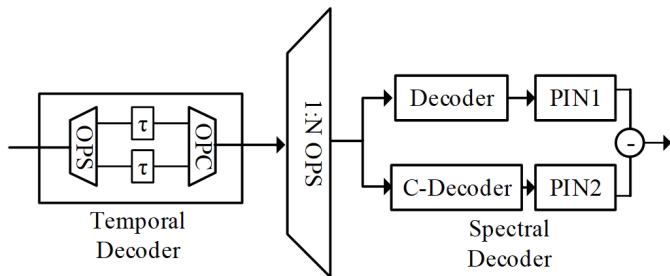


Figure 7: ONT module for the proposed architecture.

Spectral decoder primarily houses a complementary subtraction detection schemes (CSD) otherwise known as balanced detector. CSD decoder for 2D-DZ coding schemes employs 1:2 optical power splitter, which is used to splits the temporal decoded signal into two equal portions. One split portion is connected to the filter arrangement in upper leg of the CSD decoder named as Decoder. Arranging the filters in this arrangement provides maximum auto correlation, eliminating cross-correlation between the adjacent codes for the desired user. Lower leg of the decoding arrangement employs a combination of bandpass filters that are configured in complement to that of the encoder. In other words, lower leg of the

CSD decoder for user 1 will extract the spectrum that is in compliment with the X_1 code sequence.

Output of both filters are applied to the individual PIN photodiodes that converts the decoded spectrum from optical-to-electrical domain. The converted signals are then subtracted through a subtraction module to alleviate the noise factor and extract a signal with maximum autocorrelation and zero for the interfering users.

Figure 8 demonstrates the completed proposed network architecture that is developed by the application of 2D-DZ coding scheme. It can be observed that a hybrid network architecture is employed to further enhance the performance of the OCDMA system based on 2D-DZ code. Moreover, spectral and temporal encoding is performed inside the OLT modules, whereas spectral and time-based decoding is performed at the receiver module that is ONU.

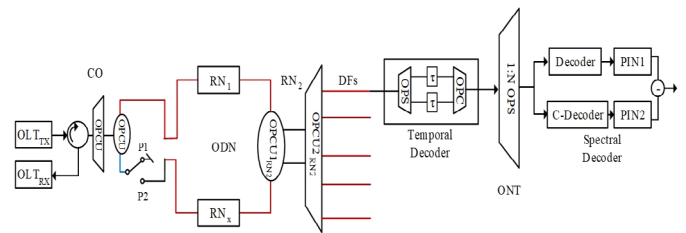


Figure 8: Proposed network architecture with OLT optical line terminal, OPCU optical power coupler, RN remote node, OPS optical power splitter, OPC optical power combiner, τ time delay units.

Performance analysis

In this evaluation the proposed system is analyzed for performance parameters under various test cases such as BER and SNR values produced in the photodiode at the receiving end. The quality of the received spectrum is effected due to the deteriorated signal to noise ratio at the receiving end noise sources. Consequently, the analysis determines SNR through Gaussian approximation followed by the implementation of BER through the given equation.

$$BER = \frac{1}{2} \operatorname{erfc} \left(\sqrt{\frac{SNR}{8}} \right)$$

Basic equation of the SNR referred to the analysis which states that $SNR = \text{Average signal power} / \text{Noise Power}$. The given equation can be further elaborated as:

$$SNR = \frac{I_{in}^2}{\sigma_{ntotal}^2} \dots (7)$$

For noise source with approximately Gaussian distribution, variance of the total noise under 2D-DZ code can be written as:

$$\langle \sigma_{ntotal}^2 \rangle = \langle \sigma_{shot}^2 \rangle + \langle \sigma_{PIIN}^2 \rangle + \langle \sigma_{th}^2 \rangle \dots (8)$$

Where; $\sigma_{shot}^2 = I^2 B \tau$ represents the shot noise power, $\sigma_{PIIN}^2 = 2eIB$ gives the IN noise power, whereas power of the thermal noise is given by $\sigma_{th}^2 = 4K_b T_n B / R_N$. Here I demonstrates the average of the total photocurrents received at the PIN photodiode. B represents the electrical bandwidth, e is the charge of electron, K_b is Boltzmann's constant, T_n is the absolute temperature, and R_N is the load resistance. For further investigations the coherent time τ can be written as:

$$\tau = \int_0^\infty G^2(v) dv / [G(v) dv]^2$$

If $G(v)$ shows single sideband power spectral density (PSD) for the optical source, then the power spectral density (PSD) for the received optical signals can be written as:

$$G(v) = \frac{P_{rd}}{w_{DEU} \Delta v} \sum_{k=0}^K d(k) \sum_{i=0}^{L_{ZCC}-1} \sum_{j=0}^{L_{DEU}-1} e_{i,j}(k) u(v, i) \dots (9)$$

Here P_{rd} is power received at the PIN photodiode, w_{DEU} and w_{ZCC} are the 2D code weights, K is the total number of subscribers in the system. L_{ZCC} and w_{DEU} demonstrates the lengths for spectral and temporal coding schemes with K^{th} user code word given as $e_{i,j}$. $u(v, i)$ represents the unit step function that can be expressed as:

$$u(v) = \begin{cases} 1, & v \geq 0 \\ 0, & v < 0 \end{cases} \dots (10)$$

Now total PSDs for the encoded spectrums received at the photodiode 0 and 2 for $d(k) = 1$ for worst case can be expresses as:

$$G_0(v) = \frac{P_{rd}}{w_{DEU} \Delta v} \sum_{k=1}^K d(k) \sum_{i=0}^{L_{ZCC}-1} \sum_{j=0}^{L_{DEU}-1} e_{i,j}^{(0)} e_{i,j}(k) u(v, i) \dots (11)$$

$$G_1(v) = \frac{P_{rd}}{(w_{DEU} - 1)w_{DEU} \Delta v} \sum_{k=1}^K d(k) \sum_{i=0}^{L_{ZCC}-1} \sum_{j=0}^{L_{DEU}-1} e_{i,j}^{(1)} e_{i,j}(k) u(v, i) \dots (12)$$

Now the total currents received at both the photodiodes can be determines as:

$$I_{PD_0} = \mathcal{R} \int_0^\infty G_0(v) dv = \frac{\mathcal{R} P_{rd}}{w_{DEU} \Delta v} \int_0^\infty \sum_{k=1}^K d(k) \sum_{i=0}^{L_{ZCC}-1} \sum_{j=0}^{L_{DEU}-1} e_{i,j}^{(0)} e_{i,j}(k) u(v, i) dv \dots (13)$$

Now by using the correlation properties for the proposed 2D-DZ codes, the above equation can be simplified for total current at photodiode 0 as:

$$I_{PD_0} = \frac{\mathcal{R} P_{rd}}{N_{ZCC} w_{ZCC}} \left[w_{ZCC} w_{DEU} + w_{ZCC} \frac{(K-1)(L_{DEU}-1)}{L_{ZCC} L_{DEU}-1} \right] \dots (14)$$

Similarly, for the second photodiode, the total current becomes.

$$I_{PD_1} = \mathcal{R} \int_0^\infty G_1(v) dv = \frac{\mathcal{R} P_{rd}}{w_{ZCC} (w_{DEU} - 1) \Delta v} \int_0^\infty \sum_{k=1}^K d(k) \sum_{i=0}^{L_{ZCC}-1} \sum_{j=0}^{L_{DEU}-1} e_{i,j}^{(1)} e_{i,j}(k) u(v, i) dv$$

Above equation can be further simplified as:

$$I_{PD_1} = \frac{\mathcal{R} P_{rd}}{w_{DEU} N_{ZCC} w_{ZCC}} \left[w_{ZCC} \frac{(K-1)(L_{DEU}-1)}{N_{ZCC} L_{DEU}-1} \right] \dots (15)$$

$$\mathcal{R} = \frac{\lambda e}{h V_c} \dots (16)$$

Now the received current's average output is calculated as follows.

$$I = \mathcal{R} \int_0^\infty [G_0(v) - G_1(v)] dv$$

Now by utilizing values of $G_0(v), G_1(v)$ from above calculations, the average output current becomes.

$$I = \frac{\mathcal{R} P_{rd}}{N_{ZCC}} \dots (17)$$

For variance of the IN's current $\langle i_{PIN}^2 \rangle = B P^2 \int_0^\infty [G_0 G_1]^2 dv / [\int_0^\infty [G_0 G_1]^2 dv]^2$ can be simplified as:

$$\langle i_{PIIN}^2 \rangle = B \mathcal{R}^2 \int_0^\infty [(G_0 - G_1)^2] dv \dots (18)$$

Now the power incidence on $G_0^2(v), G_1^2(v)$ at the receiving photodiode can be written as.

$$\int_0^\infty G_0^2(v) dv = \frac{P_{rd}^2}{w_{DEU}^2 \Delta v^2} \int_0^\infty \left[\sum_{k=1}^K d(k) \sum_{i=0}^{L_{ZCC}-1} \sum_{j=0}^{L_{DEU}-1} e_{i,j}^{(0)} e_{i,j}(k) u(v, i) \right]^2 dv$$

The above equation can be further simplified as:

$$\int_0^\infty G_0^2(v)dv = \frac{N_{ZCC}I_{PD0}^2}{R^2\Delta v} \dots (19)$$

Similarly,

$$\int_0^\infty G_1^2(v)dv = \frac{P_{rd}^2}{(w_{DEU}-1)^2w_{DEU}^2\Delta v^2} \int_0^\infty \left[\sum_{k=1}^K d(k) \sum_{i=0}^{L_{ZCC}-1} \sum_{j=0}^{L_{DEU}-1} e_{i,j}^{(1)} e_{i,j}(k)u(v,i) \right]^2 dv$$

$$\int_0^\infty G_1^2(v)dv = \frac{N_{ZCC}I_{PD1}^2}{R^2\Delta v} \dots (20)$$

Now

$$\int_0^\infty G_0(v)G_1(v)dv = \frac{P_{rd}^2}{w_{DEU}^2(w_{DEU}-1)\Delta v^2} \int_0^\infty \left[\sum_{k=1}^K d(k) \sum_{i=0}^{L_{ZCC}-1} \sum_{j=0}^{L_{DEU}-1} e_{i,j}^{(0)} e_{i,j}(k)u(v) \right] \left[\sum_{k=1}^K d(k) \sum_{i=0}^{L_2-1} \sum_{j=0}^{L_1-1} e_{i,j}^{(1)} e_{i,j}(k)u(v) \right] dv$$

By using the afore-mentioned values, above equation can be calculated as:

$$\int_0^\infty G_0(v)G_1(v)dv = \frac{N_{ZCC}I_{PD0}I_{PD1}}{R^2\Delta v} \dots (21)$$

Substituting equations (19, 20, and 21) in the equation 18, the variance of the PIIN current can be written as:

$$\langle i_{PIIN}^2 \rangle = B\mathcal{R}^2 \left[\frac{N_{ZCC}I_{PD0}^2}{R^2\Delta v} + \frac{N_{ZCC}I_{PD1}^2}{R^2\Delta v} - 2 \frac{N_{ZCC}I_{PD0}I_{PD1}}{R^2\Delta v} \right] = \frac{B\mathcal{R}^2P_{rd}^2}{N_2\Delta v} \dots (22)$$

Provided “1” and “0” are sent with equal probability for every user, Equation 22 can be further revised as:

$$\langle i_{PIIN}^2 \rangle = \frac{B\mathcal{R}^2P_{rd}^2}{2N_2\Delta v} \dots (23)$$

The variance of shot noise current is given as follows:

$$\langle i_{shot}^2 \rangle = 2eBI = 2eB[I_{PD0} + I_{PD1}] \dots (24)$$

Then

$$\langle i_{shot}^2 \rangle = \frac{2eBRP_{rd}}{w_{DEU}N_{ZCC}w_{ZCC}} \left[w_{ZCC}w_{DEU} + w_{ZCC} \frac{2(K-1)(L_{DEU}-1)}{N_{ZCC}L_{DEU}-1} \right] \dots (25)$$

Furthermore, if “1” and “0” are sent with same probability, so:

$$\langle i_{shot}^2 \rangle = \frac{eBRP_{rd}}{w_{DEU}N_{ZCC}w_{ZCC}} \left[w_{DEU}w_{ZCC} + w_{ZCC} \frac{2(K-1)(L_{DEU}-1)}{N_{ZCC}L_{DEU}-1} \right] \dots (26)$$

The thermal noise is given as:

$$\langle i_{thermal}^2 \rangle = \frac{4K_bT_nB}{R_N} \dots (27)$$

SNR for 2D-DZ system becomes:

SNR

$$= \frac{\left[\frac{BRP_{rd}}{N_{ZCC}} \right]^2}{\frac{BR^2P_{rd}^2}{2N_{ZCC}\Delta v} + \frac{eBRP_{rd}}{w_{DEU}N_{ZCC}w_{ZCC}} \left[w_{ZCC}w_{DEU} + w_{ZCC} \frac{2(K-1)(L_{DEU}-1)}{N_{ZCC}L_{DEU}-1} \right] + \frac{4K_bT_nB}{R_N}} \dots (28)$$

Results and Discussion

Figure 9 demonstrate performance of the proposed coding scheme by utilizing SNR and BER equations derived for 2D-DZ code in Section 4. Performance evaluation if made for different number of subscribers with system parameters given as Table 6. Moreover, N_{DEU} and N_{ZCC} refers to N_1 and N_2 with reference to the previous analysis. BER curves in Figure 9 shows that increasing the number of users multiple access interference (MAI) increases therefore, the performance of the system will degrade. Consequently, quality of the received signal decreases that results with the increase in BER.

Table 6: Performance parameters for system analysis.

Performance parameters	Values
LED spectral width	30 nm
Filters bandwidth	1.2 nm
Bit sequence length	128 bits
Samples per bit	64
Data rate	Variable
Signaling format	NRZ
Photodiode responsivity	1 A/W
Thermal noise	1e-22 W/Hz
Shot noise	Enabled
Dark current	10 nA
SMF wavelength	1550 nm
SMF dispersion	18 ps/nm/km
Attenuation	0.25 dB/km
Nonlinear parameters	Active
EDFA gain	20 dB

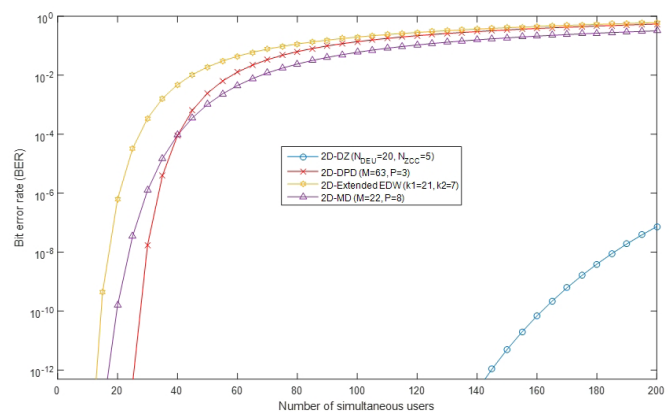


Figure 9: BER vs. number of active users for at data rate of 1.25 Gbit/s.

Moreover, Figure 9 also shows efficient performance of 2D-DZ coding scheme w.r.t the other 2D coding schemes. Furthermore, 2D-DZ offers zero cross-correlation at the V^{th} coding scheme which significantly improves the orthogonality between the adjacent codes. Moreover, utilization of zero cross-correlation codes also simplifies the receiver architecture through the use of single balanced detector arrangement which also reduces the noise at the receiving end. Therefore, the proposed technique promises performance in terms of lower BER w.r.t existing coding schemes.

Figure 10 demonstrates performance of the proposed scheme by considering the effects of received power on BER. Received power translates the signal to noise ratio at the receiving photodiode. For example more power at the receiving end generates a signal with high power in comparison to the noise sources, which reduce the contribution of noise and elevates the signal quality at the receiving photodiode. In Figure 10 it can be observed that lowering the power received at the PIN Photodiode the value of BER increases which validates the mathematical formulism and performance of the system.

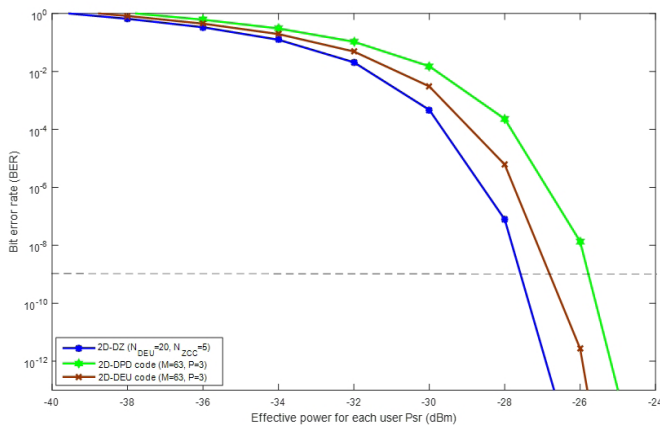


Figure 10: BER versus effective source power considering all noises at the data rate 1.25 Gbps.

It can also be observed that 2D-DZ code offer better performance in comparison with the existing coding scheme. As mentioned earlier, the proposed code facilitates the use of a single balanced detector to recover the signal which decreases signal noise for fewer receiving photodiodes. Consequently, the proposed code offers better performance in terms of BER in comparison with the existing schemes.

It can be observed in Figure 11 the system performance w.r.t BER and data rate in reference to Table 6. BER increases for higher data rates and the system

based on 2D-DZ code provides efficient correlation properties with the proposed code. This analysis also suggests the signal recovery can be achieved for maximum auto correlation and zero cross correlation with minimum components used. Thus providing efficient performance in comparison with the existing coding schemes.

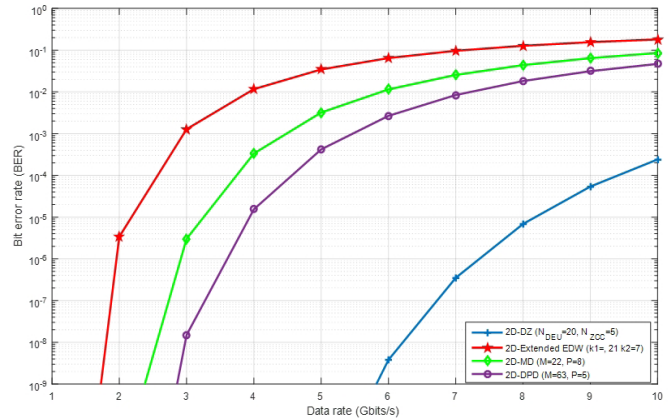


Figure 11: Data vs. bit error rate considering all noise sources.

Proof of concept

This section validates the proposed 2D-DZ based spectral/temporal OCDMA system through implementation and analysis in OptiSystem software. Implementation is performed with reference to the network architecture discussion in Section 4. All system components are placed in accordance with the implementation model in Figure 8. Moreover, the analysis is performed for 64 subscribers with $N_{DEU} = 16$ and $N_{ZCC} = 4$ communicating at different rates while using system performance parameters in Table 6.

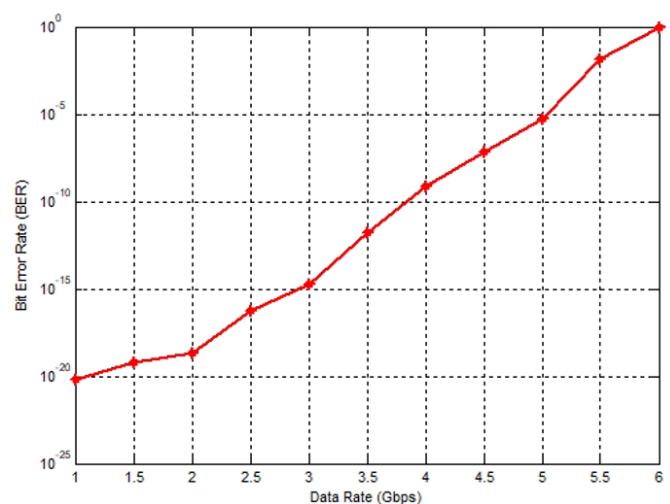


Figure 12: BER vs Data Rate for 64 subscribers with $N_{DEU} = 16$ and $N_{ZCC} = 4$.

Figure 12 demonstrates the BER w.r.t data rates for the simultaneous access of the medium by various

subscribers. It can be seen that the amount of BER increases with increase in the data transmitted across the medium. This validates the simulation model and shows that the system is performing in proximity with the analytic analysis. Furthermore, the BER is increases for higher data rate.

As mentioned in the previous section decreasing the pulsewidth with reference to the increase in data risks the system w.r.t distortion in the medium. Consequently, increasing the subscriber's communicating data rates will increase the BER. Whereas the simulation model performance shows similar pattern of decreased BER for higher data sent. Here it can be endorsed that several components parameters are accounted for in the simulation analysis that are not included in the analytic approximation. Therefore, performance is deteriorated in comparison with results obtained from the mathematical formulism. From this observation this system can support higher data rates that can transmit the data up to a distance of 25 kilometers on SMF between sender and receivers.

Conclusions and Recommendations

In this manuscript, a new encoding scheme is presented utilizing two-dimensional DEU and ZCC codes for Optical CDMA based high capacity Passive Optical Network ensuring high capacity and minimum system complexity. The proposed code is designed by the combination of 1D DEU and ZCC codes along the spectral and temporal domain. Analysis of the proposed scheme using Gaussian approximation shows that utilization of DEU code along with X^{th} domain and ZCC code along the Y^{th} axis significantly elevates orthogonality between adjacent codes and helps in signal recovery with ideal correlation properties at relatively simple components. This not only enhances the transmission capacity of the overall system but the simplified architecture of 2D-DZ OCDMA system marks it better than other schemes for the low-cost GPONs.

Novelty Statement

2D-OCDMA systems are implemented by utilizing different code combinations to offer the best correlation properties along with code length and weight. Novelty in this work is the utilization of DEU code and ZCC code to construct the two dimensional spectral/ temporal OCDMA system which has never

been done before. Furthermore, implementation of the proposed encoder and decoder in ring topology is also a novel contribution to the literature.

Author's Contribution

Mansoor Qadir: Conceived the original idea, devised the methodology, developed the theory and performed, analyzed the data, performed the experiments and wrote the manuscript.

Yousaf Khan: Supervised the study and helped in conceiving and planning the experiments.

Shahid Khan: Helped in carrying out the results, performed the analytical calculations and helped in carrying out the simulations.

Djamaledine Djeldji: Performed the numerical simulations, helped in carrying out the simulations, helped in mathematical calculations and deriving the model.

Muhammed Ismael Ibrahim Al Firas: Interpretation of the results, co-supervised the project, discussed the results and contributed to the final manuscript, critical feedback and helped shape the research.

Conflict of interest

The authors have declared no conflict of interest.

References

- Abdullah, A.R., S.A. Aljunid, A.M. Safar, J.M. Nordin and R.B. Ahmad. 2012. Mitigation of multiple access interference using two-dimensional modified double weight codes for optical code division multiple access systems. *Opt. Eng.*, 51(6): 065007. <https://doi.org/10.1117/1.OE.51.6.065007>
- Ahmed, H.Y. and K.S. Nisar. 2013. Diagonal Eigenvalue Unity (DEU) code for spectral amplitude coding-optical code division multiple access. *Opt. Fiber Technol.*, 19(4): 335-347. <https://doi.org/10.1016/j.yofte.2013.04.001>
- Ahmed, H.Y., M. Zeghid, A.W. Imtiaz, T. Sharma, A. Chehri and P. Fortier. 2020. Two-dimensional permutation vectors'(PV) code for optical code division multiple access systems. *Entropy*, 22(5): 576. <https://doi.org/10.3390/e22050576>
- Ahmed, H.Y., M. Zeghid, W.A. Imtiaz and A. Sghaier. 2019. Two dimensional Fixed Right Shift (FRS) code for SAC-OCDMA systems. *Opt. Fiber Technol.*, 47: 73-87. <https://doi.org/10.1016/j.yofte.2019.04.001>

- [org/10.1016/j.yofte.2018.11.021](https://doi.org/10.1016/j.yofte.2018.11.021)
Ahmed, H.Y., M. Zeghid, W.A. Imtiaz, Y. Sharief and A. Sghaier. 2019. A tradeoff for dispersion compensating fibers (DCFs) deployment in SAC-OCDMA environment using 2D-Fixed Right Shift (2D-FRS) code. *Optik*, 185: 746-758. <https://doi.org/10.1016/j.ijleo.2019.04.011>
- Anuar, M.S., S.A. Aljunid, N.M. Saad and S.M. Hamzah. 2009. New design of spectral amplitude coding in OCDMA with zero cross-correlation. *Opt. Commun.*, 282(14): 2659-2664. <https://doi.org/10.1016/j.optcom.2009.03.079>
- Azizoglu, M., Salehi, J.A. and Li, Y., 1992. Optical CDMA via temporal codes. *IEEE Trans. Commun.*, 40(7): 1162-1170. <https://doi.org/10.1109/26.153360>
- Ghafouri-Shiraz, H., M.M. Karbassian. 2012. *Optical CDMA networks: principles, analysis and applications*. John Wiley and Sons 4. <https://doi.org/10.1002/9781119941330>
- Imtiaz, W.A., H. Yousef, M. Zeghid, T. Sharma and J. Mirza. 2020. Techno-economic analysis of two dimensional optical code division multiple access systems. *Opt. Quant. Electron.*, 53: 1-5. <https://doi.org/10.1007/s11082-020-02630-z>
- Imtiaz, W.A., H.Y. Ahmed, M. Zeghid and Y. Sharief. 2020. An optimized architecture to reduce the impact of fiber strands in spectral/spatial optical code division multiple access passive optical networks (OCDMA-PON). *Opt. Fiber Technol.*, 54: 102072. <https://doi.org/10.1016/j.yofte.2019.102072>
- Imtiaz, W.A., H.Y. Ahmed, M. Zeghid, Y. Sharief and M. Usman. 2019. Design and implementation of two-dimensional enhanced multi-diagonal code for high cardinality OCDMA-PON. *Arab. J. Sci. Eng.*, 44(8): 7067-7084. <https://doi.org/10.1007/s13369-019-03789-8>
- Jellali, N., M. Najjar, M. Ferchichi and H. Rezig. 2017. Development of new two-dimensional spectral/spatial code based on dynamic cyclic shift code for OCDMA system. *Opt. Fiber Technol.*, 36: 26-32. <https://doi.org/10.1016/j.yofte.2017.02.002>
- Kadhim, R.A., H.A. Fadhil, S.A. Aljunid and M.S. Razalli. 2014. A new two dimensional spectral/spatial multi-diagonal code for noncoherent optical code division multiple access (OCDMA) systems. *Opt. Commun.*, 329: 28-33. <https://doi.org/10.1016/j.optcom.2014.04.082>
- Kandouci, C., A. Djebbari and A. Taleb-Ahmed. 2017. A new family of 2D-wavelength-time codes for OCDMA system with direct detection. *Optik*, 135: 8-15. <https://doi.org/10.1016/j.ijleo.2017.01.065>
- Keraf, N.D., S.A. Aljunid, A.R. Arief and P. Ehkan. 2015. The evolution of double weight codes family in spectral amplitude coding OCDMA. *Adv. Comput. Commun. Eng. Technol.*, Springer, Cham. pp. 129-140. https://doi.org/10.1007/978-3-319-07674-4_14
- Koonen, T., 2006. Fiber to the home/fiber to the premises: what, where, and when? *Proc. IEEE*. 94(5): 911-934. <https://doi.org/10.1109/JPROC.2006.873435>
- Kumawat, S., m.R. Kumar and S.J. Nanda. 2D code construction using DW code families for SAC-OCDMA systems. In *TENCON 2017-2017 IEEE Region 10 Conference 2017 Nov 5*. IEEE. pp. 2451-2455. <https://doi.org/10.1109/TENCON.2017.8228273>
- Lam, C.F., 2011. *Passive optical networks: Principles and practice*. Elsevier,
- Lee, T.S., H.M. Shalaby and Ghafouri-Shiraz, H., 2001. Interference reduction in synchronous fiber optic PPM-CDMA systems. *Microw. Opt. Technol. Lett.*, 30(3): 202-205. <https://doi.org/10.1002/mop.1265>
- Mahloo, M., 2013. Reliability versus cost in next generation optical access networks. Doctoral dissertation, KTH Royal Institute of Technology.
- Najjar, M., N. Jellali and M. Ferchichi. 2017. Two-dimensional multi-service code for spectral/spatial optical CDMA system. *Opt. Quant. Electron.*, 49(12): 397. <https://doi.org/10.1007/s11082-017-1234-x>
- Najjar, M., N. Jellali, M. Ferchichi and H. Rezig. 2017. Spectral/spatial optical CDMA code based on diagonal eigenvalue unity. *Opt. Fiber Technol.*, 38: 61-69. <https://doi.org/10.1016/j.yofte.2017.08.003>
- Nisar, K.S., 2014. Construction of zero cross correlation code using a type of anti-diagonal-identity-column block matrices. *Optik*, 125(21): 6586-6588. <https://doi.org/10.1016/j.ijleo.2014.07.068>
- Qadir, M., Y. Khan and M. Alfrass. 2020. Enhancing system capacity for 2d spectral temporal optical code division multiple access systems. *J. Mech.*

- Continua Math. Sci., 15(1): 283-290. <https://doi.org/10.26782/jmcms.2020.01.00022>
- Sahbudin, R.K., M. Kamarulzaman, S. Hitam, M. Mokhtar and S.B. Anas. Performance of SAC OCDMA-FSO communication systems. Opt. Int. J. Light Electron. Opt., 124(17): 2868-2870. <https://doi.org/10.1016/j.ijleo.2012.08.067>
- Sahraoui, W., A. Amphawan, S. Berrah and R. Matem. 2020. A novel 2D polarization-spatial encoding approach for OCDMA system based on multi-core fiber. Optik, 18: 166164. <https://doi.org/10.1016/j.ijleo.2020.166164>
- Shi, F. and Ghafouri-Shiraz, H., 2016. Performance Analysis of two new code families for spectral-amplitude-coding optical CDMA systems. J. Lightw. Technol., 34(17): 4005-4014. <https://doi.org/10.1109/JLT.2016.2586527>
- Singh, H., A. Sheetal and M. Singh. 2016. Performance analysis of 2D Multi-diagonal code for OCDMA system. Int. Res. J. Eng. Technol., 3(5): 1282-1287.
- Wei, Z., H.M. Shalaby, H. Ghafouri-Shiraz. 2001. Modified quadratic congruence codes for fiber Bragg-grating-based spectral-amplitude-coding optical CDMA systems. J. Lightw. Technol., 19(9): 1274-1281. <https://doi.org/10.1109/50.948274>
- Yin, H. and D.J. Richardson. 2009. Two-Dimensional OCDMA Codes. Optical Code Division Multiple Access Communication Networks: Theory and Applications. 2009: 97-167.